Magic Clusters PtMg$_{2,3}$H$_5^-$ Facilitated by Local σ-Aromaticity

Wei Wang,[a] Jie Wang,[a] Chu Gong,[a] Zhaoguo Zhu,[b] Kit H. Bowen,*[b] and Xinxing Zhang*[a]

The concept of local aromaticity has been successfully utilized in understanding the stability of certain atomic clusters. However, all the skeleton atoms in these clusters are covered by at least one local aromatic feature, collectively making the multiple local aromaticities coexist globally. Herein we show the robustness of local aromaticity as a tool for the discovery of novel magic clusters: not all of the skeleton atoms need to be covered by an aromatic feature to make the cluster magic. In this study, the PtMg$_{2,3}$H$_5^-$ cluster anions are generated by a unique high-current pulsed discharge ion source and found to be magic numbers using mass spectrometry. Photoelectron spectroscopy and calculations confirm that only the PtH$_4^{2-}$ kernels in these clusters are locally aromatic. Based on these results, we propose that local aromaticity can be gainfully utilized as a new potential magic rule in the search for magic numbers.

Local aromaticity, the aromaticity that only covers part of the atoms in a molecule, has been widely exploited and combined with traditional global aromaticity to understand the relative stability of polycyclic aromatic hydrocarbons (PAHs), and to validate the Clar's model of the aromatic π-sextet rule.[1–7] A plethora of indices have been developed to gain insights into local aromaticity, among which both good correlations and discrepancies coexist.[4–7] Recently, Boldyrev and coworkers developed a unique theoretical tool, the adaptive natural density partitioning (AdNDP) method,[8] to analyze the partitioning of the charge density into the atoms of a molecule or cluster with the highest possible degree of localization of electron pairs. With AdNDP they have successfully investigated and visualized the coexistence of localized and global aromaticities in PAHs.[9–10] Remarkably, using the same approach, they opine that global aromaticity does not exist in graphene, the poster child of big π-conjugated systems.[11] Instead, each of the hexagonal rings of graphene contains two π electrons (each carbon atom of the six atoms in a ring is shared by three

adjacent rings), yielding local aromaticity of $4n+2$ ($n=0$) in every ring.

Based on the atomic orbitals from which they are formed and the number of nodal planes, various types of aromaticities, e.g., σ-, π-, and δ-aromaticity, have also been utilized to understand the stabilities of atomic clusters[12–20] in addition to those of PAHs. In some cases, multiple aromaticities were found to coexist, facilitating the observations of unusually stable species.[17–20] Nevertheless, cluster stability was, in most cases, the result of global aromaticity, with examples of high stability due to local aromaticity being extremely scarce. Examples include Li$_4$ and B$_6^{2-}$ which contain multiple localized aromatic characters that cover all the atoms in the clusters.[8,13] More recently, Boldyrev et al. reported that the widely-used non-agermanide Ge$_9^{4-}$ Zintl anion in inorganic synthesis possesses unique multiple local σ-aromaticity, explaining the high stability and wide applications of this cluster.[21] In Li$_4$, B$_6^{2-}$, Ge$_9^{4-}$, and in the extreme case of graphene,[11] the multiple local aromaticities make the overall aromaticity global. Stated alternatively, all the skeleton atoms in these examples are covered by at least one local aromatic feature. Intuitively, such scenario guarantees the stability of these systems.

In view of the above discussions, we raise the following questions: if a cluster is not globally covered by multiple local aromaticity, namely, if not all of the skeleton atoms are endowed with at least one aromatic character, can it still be a magic cluster? How far can we stretch the applicability of local aromaticity in the discovery of new stable clusters?

To answer the above questions experimentally, we used a combination of mass spectrometric and anion photoelectron spectroscopic (PES) methods to investigate the PtMg$_2$H$_5^-$ and PtMg$_3$H$_5^-$ cluster anions generated by a unique high-current pulsed arc cluster ionization source (PACIS). Details of the experimental methods and the apparatus are provided in the Supporting Information (SI). Figure 1 shows the mass spectra of the experimental and simulated natural isotopic distributions of PtMg$_{2,3}$H$_5^-$. It is seen that both spectra match very well not only in the isotopic distributions, but also in the relative intensities of their isotopomers. Also, only nominal ion signals from PtMg$_{2,3}$H$_n^-$ (n < 5) are observed on the low m/z side of each of the isotopic groups in the experiment. This phenomenon is uncommon for mass spectrometric studies of metal hydrides, since there are almost always diverse combinations of hydrogen atoms attached to the metal atoms as shown in previous reports.[22–24] When a cluster ion exhibits unusually high intensity relative to its neighbors in the mass spectrum, it might well possess some particular property that facilitates its abundance and by implication, its stability. Clusters of this type are often declared the "magic clusters",[25] and examples of such clusters include the famous discovery of C$_{60}$.[26]

[a] W. Wang, J. Wang, C. Gong, Prof. Dr. X. Zhang
Key Laboratory of Advanced Energy Materials Chemistry (Ministry of Education)
Renewable Energy Conversion and Storage Center (ReCAST)
College of Chemistry, Nankai University
Tianjin 300071, China
E-mail: zhangxx@nankai.edu.cn
[b] Z. Zhu, Prof. Dr. K. H. Bowen
Departments of Chemistry and Material Science
Johns Hopkins University
Baltimore, MD, 21218, USA
E-mail: kbowen@jhu.edu

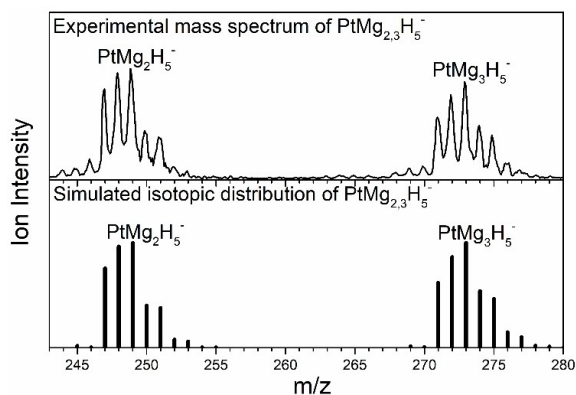Supporting information for this article is available on the WWW under https://doi.org/10.1002/cphc.202000691

ChemPhysChem

Communications
doi.org/10.1002/cphc.202000691

Chemistry Europe
European Chemical
Societies Publishing

Figure 1. Experimental and simulated isotopic distributions of $PtMg_{2,3}H_5^-$.

To further characterize these clusters, anion photoelectron spectra (Figure 2) taken with 355 nm laser were employed to study the electronic structures of $PtMg_{2,3}H_5^-$. The spectra were recorded several times on different isotopomers to avoid potential contaminations from clusters having fewer number of hydrogen atoms even though their signal is very weak in the mass spectrum. For $PtMg_2H_5^-$, a broad electron binding energy (EBE) spectral band ranges from EBE ~2.0 eV to ~3.0 eV and reaches its intensity maximum at 2.35 eV, with the latter number being its first vertical detachment energy (VDE1) value, the transition at which the Franck-Condon overlap between the
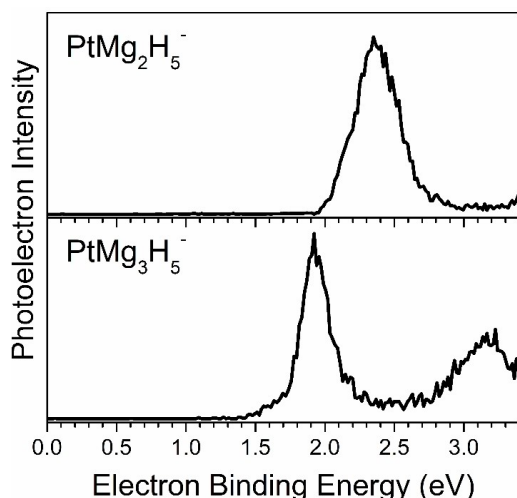
wave functions of the anion and its neutral counterpart is maximal. For $PtMg_3H_5^-$, the spectrum has two EBE bands starting from ~1.6 eV and ~2.7 eV, with these reaching their maxima at EBE = 1.91 eV and 3.22 eV, respectively, corresponding to its first and second VDE values. The second VDE (VDE2), 3.22 eV, corresponds to the vertical transition from the anion to the first excited state of the neutral with the same structure as the anion. These numbers are tabulated in Table 1 for comparison with the values obtained from the calculations.

Isolated and well-characterized gas-phase ions are ideally suited for simulations employing various quantum theoretical methods. The high complementary and comparability of experiment and theory in the case of gas-phase investigations have potential for handling challenging theoretical tasks, such as searches for global minima (GM) and chemical bonding analyses. To better understand the $PtMg_{2,3}H_5^-$ clusters, we carried out unbiased GM searches using the Coalescence Kick (CK) technique.[27] The GMs are expected to be the main contributors to the photoelectron spectra. Details on the theoretical methods are presented in the SI. Using the CK program, 10,000 trial structures (singlet and triplet) for both cluster anions underwent geometry optimizations at a less expensive level of theory, subsequently the lowest six isomeric structures were recalculated at higher levels of theory, and then ranked as Iso1 to Iso 6 according to their relative energies as shown in Figure 3. The 3D coordinates of all of the calculated species are presented in the SI. The GM of $PtMg_2H_5^-$ (Iso 1) has the Pt atom surrounded by four H atoms, while the rest Mg atom and the Mg—H moiety approach the center Pt atom from two different directions (Cs symmetry with the plane of symmetry covers the Mg—Pt-Mg triangle). The GM (Iso 1) of $PtMg_3H_5^-$ is very similar to that of $PtMg_2H_5^-$, with the third Mg atom attaching to the center Pt atom from the bottom (Cs symmetry). To verify that the GM structures of $PtMg_{2,3}H_5^-$ indeed contribute the most to the photoelectron spectra, their VDEs are computed for the comparisons with experimental values. As shown in Table 1, the calculated first one and/or two VDE values coincide with the experimental values, thus supporting the computationally predicted GM structures. While the Iso 2 of $PtMg_2H_5^-$ is significantly higher in energy than Iso 1, which often excludes its existence in the experiment, the Iso 2 of $PtMg_3H_5^-$ is only 0.11 eV higher than Iso 1. To explore whether Iso 2 of $PtMg_3H_5^-$ exists in the experiment, its VDE value was also calculated and presented in Table 1; it did not match the measured VDE value. Therefore, we conclude that only the calculated GMs of $PtMg_{2,3}H_5^-$ are observed in the experiment.

Figure 2. Photoelectron spectra of $PtMg_{2,3}H_5^-$ taken with 355 nm laser.

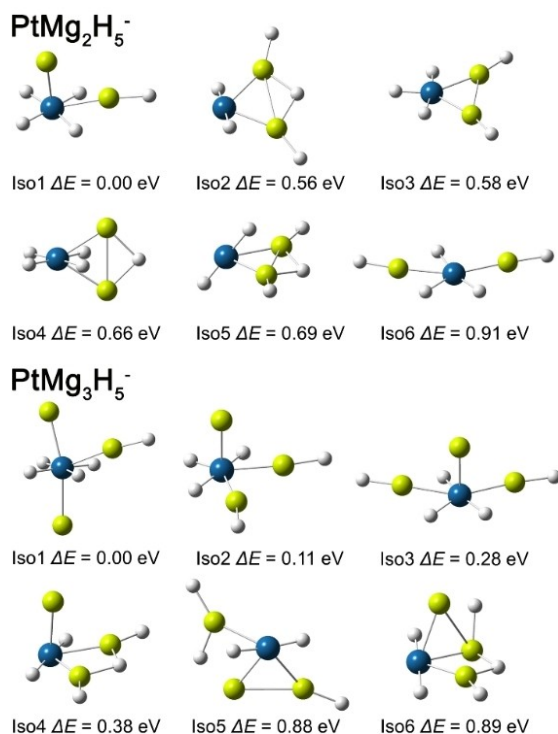| Table 1. Experimental and theoretical VDE values (in eV) for $PtMg_2H_5^-$ and $PtMg_3H_5^-$ at the PBEPBE/6-311++G(3df,3pd)/LANL2DZ level of theory.				
System	Expt. VDE1	Theo. VDE1	Expt. VDE2	Theo. VDE2
$PtMg_2H_5^-$ (isomer 1)	2.35	2.37	–	4.56
$PtMg_3H_5^-$ (isomer 1)	1.91	1.88	3.22	3.44
$PtMg_3H_5^-$ (isomer 2)	1.91	2.57	3.22	3.33

Figure 3. Lowest energy structures of PtMg$_{2,3}$H$_5^-$ and their relative energies calculated at the CCSD(T)/6-311 + +G(3df,3pd)/LanL2DZ levels of theory. All of them are in the singlet spin state. The solid rods between atoms help to visualize but do not necessarily represent σ-bonds here and elsewhere. Pt is blue, Mg is yellow, and H is white.

Figure 4. The resemblance of the σ-aromaticity in the PtH$_4^{2-}$, PtMg$_2$H$_5^-$ and PtMg$_3$H$_5^-$ clusters revealed by AdNDP analyses mapped on the 0.02 e/bohr^3 surfaces at the PBEPBE/6-311 + +G(3df,3pd)/LANL2DZ level of theory. The aromaticity of PtH$_4^{2-}$ is global, while those of PtMg$_2$H$_5^-$ and PtMg$_3$H$_5^-$ are local.

At first glance, the structures of the GMs of PtMg$_{2,3}$H$_5^-$ do not have obvious characteristics of stability like high symmetry or adherrence to the magic rules such as the 18-electron rule, the octet rule, or the jellium model[28] that are often used to discover magic clusters. To resolve this enigma, we employed the a natural population analysis (NPA) to provide the charge distributions of these clusters at the PBEPBE/6-311 + +G (3df,3pd)/LANL2DZ level of theory (Figure S1 in the Supporting Information for details). With its relatively high electronegativity, the Pt atom has the electronic configuration, 6 s$^{0.86}$5d$^{9.37}$6p$^{1.12}$ in PtMg$_2$H$_5^-$, making the Pt atom negatively charged by −1.34 e. By comparison, the Pt atom in PtMg$_3$H$_5^-$ has the electronic configuration, 6 s$^{0.91}$5d$^{9.42}$6p$^{1.71}$, making the Pt atom negatively charged by −2.05 e. As a result, the PtH$_4$ kernels in PtMg$_2$H$_5^-$ and PtMg$_3$H$_5^-$ possess negative charges of −1.69 e and −2.14 e, respectively, practically making them PtH$_4^{2-}$ moieties. The Mg atoms apparently are functioning as electron donors for the PtH$_4^{2-}$ kernels.

We next performed an AdNDP analysis[8] of the kernel, PtH$_4^{2-}$ that has a D_{4h} symmetry (Figure 4, top panel). Three 5-center 2-electron (5c–2e) σ bonds with occupation numbers (ON) of 2.00 |e| were revealed, corresponding to its σ-aromaticity, suggesting that PtH$_4^{2-}$ could be potentially utilized as a building block to construct other compounds. The σ-aromaticity is apparently global in PtH$_4^{2-}$ because it covers all of the five atoms in the cluster. Similarly, three 5c–2e σ bonds
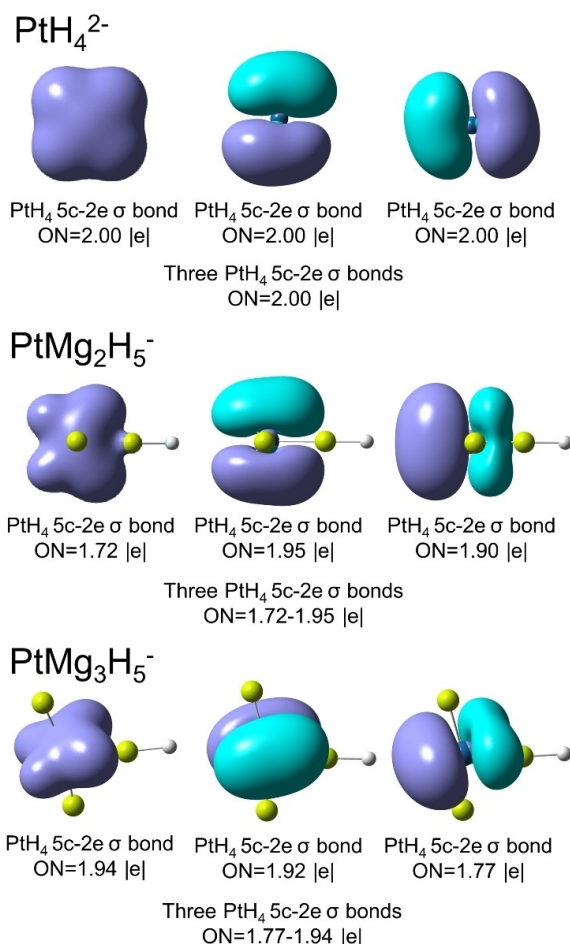
on the PtH$_4$ kernels in PtMg$_{2,3}$H$_5^-$ with high ON values ranging from 1.72 |e| to 1.95 |e| are also displayed in Figure 4, which resemble those of PtH$_4^{2-}$. The σ-aromaticity in PtMg$_{2,3}$H$_5^-$ is indeed local aromaticity because it only covers five atoms of these eight- or nine-atom clusters. The AdNDP orbitals of these three clusters at other isovalue contours are provided in Figure S2 for clarity.

To further evaluate the σ-aromaticity in these clusters, finally, we investigated the ring current density using the gauge-including magnetically induced current (GIMIC) method[29–31] for the four systems in Figure 5. As shown in Figure 5, clockwise diatropic ring current are observed around the PtH$_4$ kernels in all of the four systems, which consolidate the existence of σ-aromaticity. Ring current strengths (nA T^{-1}) are obtained by numerical integration of the current density susceptibility passing through the 2.0 Å long planes (marked as black lines in Figure 5) of the PtH$_5^-$, PtH$_4^{2-}$, PtMg$_2$H$_5^-$, and PtMg$_3$H$_5^-$ clusters. These current strength values are comparable to previously published aromatic systems.[32]
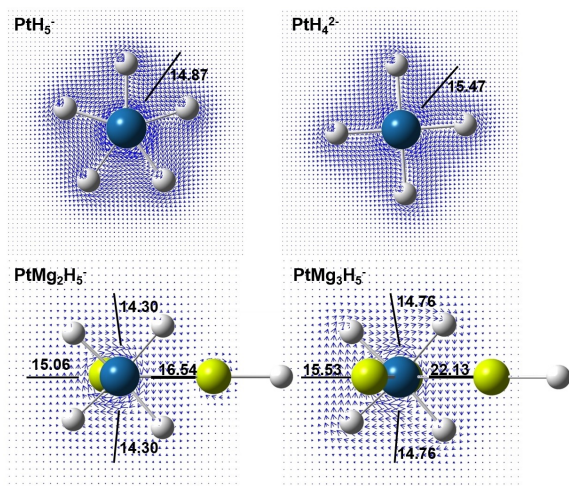
Figure 5. Magnetically-induced diatropic ring current calculated at the plane of the PtH_4 kernels with the GIMIC method. Integrated ring current strengths (nA T^{-1}) passing through the 2.0 Å long planes (black lines) are also given.

In conclusion, here we report an investigation of the structural and electronic properties, as well as the chemical bonding in the $PtMg_2H_5^-$ and $PtMg_3H_5^-$ cluster anions using a combination of mass spectrometry, anion photoelectron spectroscopy and quantum chemical calculations. The mass spectra reveal that these clusters are magic numbers. Unbiased global geometry searches found the GMs that contribute to the experimentally observed photoelectron spectra. AdNDP results indicate that $PtMg_{2,3}H_5^-$ have σ-aromaticity that resembles that of PtH_4^{2-}, with the former being local but the latter being global. While all existing examples need multiple local aromaticity to cover all of the atoms in a cluster to make them highly stable, this study identifies the first case where single local aromaticity, that does not cover all the atoms in a cluster, can nevertheless still make the whole cluster a magic number. Taken together, we have determined how far one can extend the applicability of local aromaticity in discovering new magic clusters: a single local aromatic feature that only covers part of the atoms in a cluster might already be enough. We have shown the robustness of local aromaticity as a potential new magic rule in finding exotic magic numbers, and we anticipate that more magic clusters and compounds using them as building blocks will be discovered based on the type of local aromaticity described in this work.

Acknowledgements

Conflict of Interest

The authors declare no conflict of interest.

[1] A. Moyano, J. C. Paniagua, *J. Org. Chem.* **1991**, *56*, 1858–1866.
[2] M. K. Cyrański, T. M. Krygowski, M. Wisiorowski, N. J. R. van Eikema Hommes, P. v R Schleyer, *Angew. Chem. Int. Ed.* **1998**, *37*, 177–180; *Angew. Chem.* **1998**, *110*, 187–190.
[3] M. Randić, A. T. Balaban, *Int. J. Quantum Chem.* **2018**, *118*, e25657.
[4] G. Portella, J. Poater, M. Solà, *J. Phys. Org. Chem.* **2005**, *18*, 785–791.
[5] P. Bultinck, *Faraday Discuss.* **2007**, *135*, 347–365.
[6] M. Makino, N. Nishina, J. Aihara, *J. Phys. Org. Chem.* **2018**, *31*, e3783.
[7] J. Poater, I. García-Cruz, F. Illas, M. Solà, *Phys. Chem. Chem. Phys.* **2004**, *6*, 314–318.
[8] D. Y. Zubarv, A. I. Boldyrev, *Phys. Chem. Chem. Phys.* **2008**, *10*, 5207–5217.
[9] I. A. Popov, A. I. Boldyrev, *Eur. J. Org. Chem.* **2012**, 3485–3491.
[10] D. Y. Zubarev, A. I. Boldyrev, *J. Org. Chem.* **2008**, *73*, 9251–9258.
[11] I. A. Popov, K. V. Bozhenko, A. I. Boldyrev, *Nano Res.* **2012**, *5*, 117–123.
[12] X. Li, A. E. Kuznetsov, H. F. Zhang, A. I. Boldyrev, L. S. Wang, *Science* **2001**, *291*, 859–861.
[13] I. A. Popov, A. A. Starikova, D. V. Steglenko, A. I. Boldyrev, *Chem. Eur. J.* **2018**, *24*, 292–305.
[14] X. Zhang, G. Liu, G. Gantefoer, K. H. Bowen, A. N. Alexandrova, *J. Phys. Chem. Lett.* **2014**, *5*, 1596–1601.
[15] C. S. Wannere, C. Corminboeuf, Z. -X. Wang, M. D. Wodrich, R. B. King, P. v R Schleyer, *J. Am. Chem. Soc.* **2005**, *127*, 5701–5705.
[16] Z. Chen, C. S. Wannere, C. Corminboeuf, R. Puchta, P. v R Schleyer, *Chem. Rev.* **2005**, *105*, 3842–3888.
[17] A. S. Ivanov, X. Zhang, H. Wang, A. I. Boldyrev, G. Gantefoer, K. H. Bowen, I. Cernusak, *J. Phys. Chem. A* **2015**, *119*, 11293–11303.
[18] W. Wang, J. Wang, C. Gong, C. Mu, D. Zhang, X. Zhang, *Chin. J. Chem. Phys.* DOI:10.1063/1674-0068/cjcp2004057 (2020).
[19] H. J. Zhai, A. E. Kuznetsov, A. I. Boldyrev, L. S. Wang, *ChemPhysChem* **2004**, *5*, 1885–1891.
[20] A. I. Boldyrev, L. S. Wang, *Chem. Rev.* **2015**, *105*, 3716–3757.
[21] N. V. Tkachenko, A. I. Boldyrev, *Chem. Sci.* **2019**, *10*, 5761–5765.
[22] X. Zhang, H. Wang, E. Collins, A. Lim, G. Ganteför, B. Kiran, H. Schnöckel, B. Eichhorn, K. H. Bowen, *J. Chem. Phys.* **2013**, *138*, 124303.
[23] X. Zhang, P. Robinson, G. Gantefoer, A. Alexandrova, K. H. Bowen, *J. Chem. Phys.* **2015**, *143*, 094307.
[24] X. Zhang, G. Liu, K. -H. Meiwes-Broer, G. Ganteför, K. H. Bowen, *Angew. Chem. Int. Ed.* **2016**, *55*, 9644–9647; *Angew. Chem.* **2016**, *128*, 9796–9799.
[25] I. A. Solov'yov, A. V. Solov'yov, W. Greiner, A. Koshelev, A. Shutovich, *Phys. Rev. Lett.* **2003**, *90*, 053401.
[26] H. W. Kroto, J. R. Heath, S. C. O'Brien, R. F. Curl, R. E. Smalley, *Nature* **1985**, *318*, 162–163.
[27] A. P. Sergeeva, B. B. Averkiev, H. J. Zhai, H. A. I. Boldyrev, L. S. Wang, *J. Chem. Phys.* **2011**, *134*, 224304.
[28] W. D. Knight, K. Clemenger, W. A. de Heer, W. A. Saunders, M. Y. Chou, M. L. Cohen, *Phys. Rev. Lett.* **1984**, *52*, 2141–2143.
[29] J. Jusélius, D. Sundholm, J. Gauss, *J. Chem. Phys.* **2004**, *121*, 3952–3963.
[30] S. Taubert, D. Sundholm, J. Jusélius, *J. Chem. Phys.* **2011**, *134*, 054123.
[31] H. Fliegl, F. Pichierri, D. Sundholm, *J. Phys. Chem. A* **2015**, *119*, 2344–2350.
[32] D. Sundholm, R. J. F. Berger, H. Fliegl, *Phys. Chem. Chem. Phys.* **2016**, *18*, 15934–15942.